Redundancy of *Saccharomyces cerevisiae MSH3* and *MSH6* in *MSH2*-dependent mismatch repair

Gerald T. Marsischky, Nicole Filosi, Michael F. Kane, and Richard Kolodner[1]

Charles A. Dana Division of Human Cancer Genetics, Dana-Farber Cancer Institute, Boston, Massachusetts 02115 USA; Department of Biological Chemistry and Molecular Pharmacology, Harvard Medical School, Boston, Massachusetts 02115 USA

***Saccharomyces cerevisiae* encodes six genes, *MSH1–6*, which encode proteins related to the bacterial MutS protein. In this study the role of *MSH2*, *MSH3*, and *MSH6* in mismatch repair has been examined by measuring the rate of accumulating mutations and mutation spectrum in strains containing different combinations of *msh2*, *msh3*, and *msh6* mutations and by studying the physical interaction between the MSH2 protein and the MSH3 and MSH6 proteins. The results indicate that *S. cerevisiae* has two pathways of *MSH2*-dependent mismatch repair: one that recognizes single-base mispairs and requires *MSH2* and *MSH6*, and a second that recognizes insertion/deletion mispairs and requires a combination of either *MSH2* and *MSH6* or *MSH2* and *MSH3*. The redundancy of *MSH3* and *MSH6* explains the greater prevalence of *hmsh2* mutations in HNPCC families and suggests how the role of *hmsh3* and *hmsh6* mutations in cancer susceptibility could be analyzed.**

[*Key Words*: Cancer; mutagenesis; mismatch repair; *mutS*; *MSH2*; *MSH3*; *MSH6*; *Saccharomyces cerevisiae*]

Received October 17, 1995; revised version accepted January 17, 1996.

DNA mismatch repair plays a number of roles in the cell including the repair of mispaired bases produced as a result of DNA replication errors, chemical damage to DNA and DNA precursors, processing of recombination intermediates, and suppression or regulation of recombination between divergent DNA sequences (for review, see Modrich 1991, 1994; Kolodner 1995). DNA mismatch repair is best understood in bacterial systems; however a series of genetic and biochemical studies has shown that eukaryotes contain a mismatch repair system that is similar to the bacterial MutHLS system indicating evolutionary conservation of at least some of the components of mismatch repair (Bishop et al. 1987, 1989; W. Kramer et al. 1989; Reenan and Kolodner 1992a,b; Fishel et al. 1993; Leach et al. 1993; Bronner et al. 1994; Nicolaides et al. 1994; Papadopoulos et al. 1994; Li and Modrich 1995). The recent observations that inherited mutations in mismatch repair genes cause a common human cancer susceptibility syndrome (Fishel et al. 1993; Leach et al. 1993; Bronner et al. 1994; Kolodner et al. 1994, 1995; Liu et al. 1994; Nicolaides et al. 1994; Papadopoulos et al. 1994), that acquired mismatch repair defective mutations occur in sporadic colon tumors (Borresen et al. 1995), and that many human tumor cell lines are mismatch repair defective (Parsons et al. 1993; Umar et al. 1994; Boyer et al. 1995; Liu et al. 1995) have underscored the importance of understanding mismatch repair in detail.

The yeast *Saccharomyces cerevisiae* provides an ideal system for use in understanding mismatch repair because of the availability of both genetic and biochemical methods for analyzing mismatch repair and the complete *S. cerevisiae* genome sequence, soon to be available. Analysis of *S. cerevisiae* has led to the understanding of at least three components of a bacterial MutHLS-like mismatch repair system. MSH2 is highly related to the bacterial MutS family of proteins, and as predicted by this homology, MSH2 protein can bind to mispaired bases, albeit with a higher affinity for insertion/deletion mispair than for single-base mispairs (Reenan and Kolodner 1992a,b; Alani et al. 1995). PMS1 and MLH1 are each homologs of MutL, and these two proteins form a complex that can bind to MSH2 when MSH2 is bound to a mispaired base, similar to the interaction between *Escherichia coli* MutL and MutS (Grilley et al. 1989; Kramer et al. 1989; Prolla et al. 1994a,b). Human cells contain homologs of the *S. cerevisiae* MSH2 (hMSH2), PMS1 (hPMS2), and MLH1 (hMLH1) proteins, and these proteins appear to play roles that are similar to those of their *S. cerevisiae* counterparts (Fishel et al. 1993; Leach et al. 1993; Bronner et al. 1994; Fishel et al. 1994; Nicolaides et al. 1994; Papadopoulos et al. 1994; Li and Modrich 1995). There is also evidence that the human mispair recognition complex contains a second subunit in addi-

[1]Corresponding author.

tion to MSH2, GTBP/p160, which is also a MutS homolog (Drummond et al. 1995; Palombo et al. 1995).

S. cerevisiae also contains a number of other *MSH* genes whose function is generally less understood. *MSH1* encodes a mispair binding protein that is imported into mitochondria and appears to function in mitochondrial mismatch repair (Reenan and Kolodner 1992a,b; Chi and Kolodner 1994). Mutations in *MSH3* confer a weak nuclear mutator phenotype in some mutator assays (New et al. 1993; Alani et al. 1994; Strand et al. 1995). However, the magnitude of these effects is substantially less than those caused by mutations in *MSH2*, *PMS1*, or *MLH1*, suggesting that MSH3 may play a relatively minor role in mismatch repair (Williamson et al. 1985; Reenan and Kolodner 1992a; New et al. 1993; Alani et al. 1994; Prolla et al. 1994a; Strand et al. 1995). *MSH4* and *MSH5* do not appear to function in mismatch repair but rather have a role in meiotic recombination (Ross-Macdonald and Roeder 1994; Hollingsworth et al. 1995). In this study we describe a sixth *MSH* gene, *MSH6*, and present results that demonstrate that *MSH2*, *MSH3*, and *MSH6* all play important roles in mismatch repair.

Results

Identification of MSH

To identify additional *MSH* genes, the *S. cerevisiae* Genome Database was searched for protein sequences showing homology to the most conserved region of MSH2 (Reenan and Kolodner 1992b; Fishel et al. 1993). One new gene encoding such a protein was identified and called *MSH6*. This gene was predicted to encode a 139,992 molecular weight protein, showed homology along its entire length with *E. coli* MutS and *S. cerevisiae* MSH2 (Fig. 1A), and had an amino acid identity of 18.5% and 18.1% with these two proteins, respectively.

After the studies described here had been partially completed, we became aware of the identification of the human *GTBP* gene by J. Jiricny (Instituto Di Richerche Di Biologia Moleculare P. Angeletti, Rome, Italy) and collaborators. Regions of protein sequence identity between *S. cerevisiae* and mouse MSH6 (G. Crouse and R. Kolodner, unpubl.) were provided to J. Jiricny, who found that they exactly matched regions of the human GTBP amino acid sequence. When larger amounts of the human GTBP amino acid sequence became available (Palombo et al. 1995), sequence alignments (Fig. 1B) demonstrated that *S. cerevisiae* MSH6 and human GTBP were related more closely to each other than to any other MutS homolog (26.6% amino acid identity).

MSH6 is involved in DNA repair

To determine whether *MSH6* is involved in DNA repair, *MSH6* was disrupted in a diploid strain, which was then sporulated and analyzed by tetrad analysis. In all cases (27 spore clones analyzed) *msh6* mutations cosegregated with a mutator phenotype as assessed in patch tests that

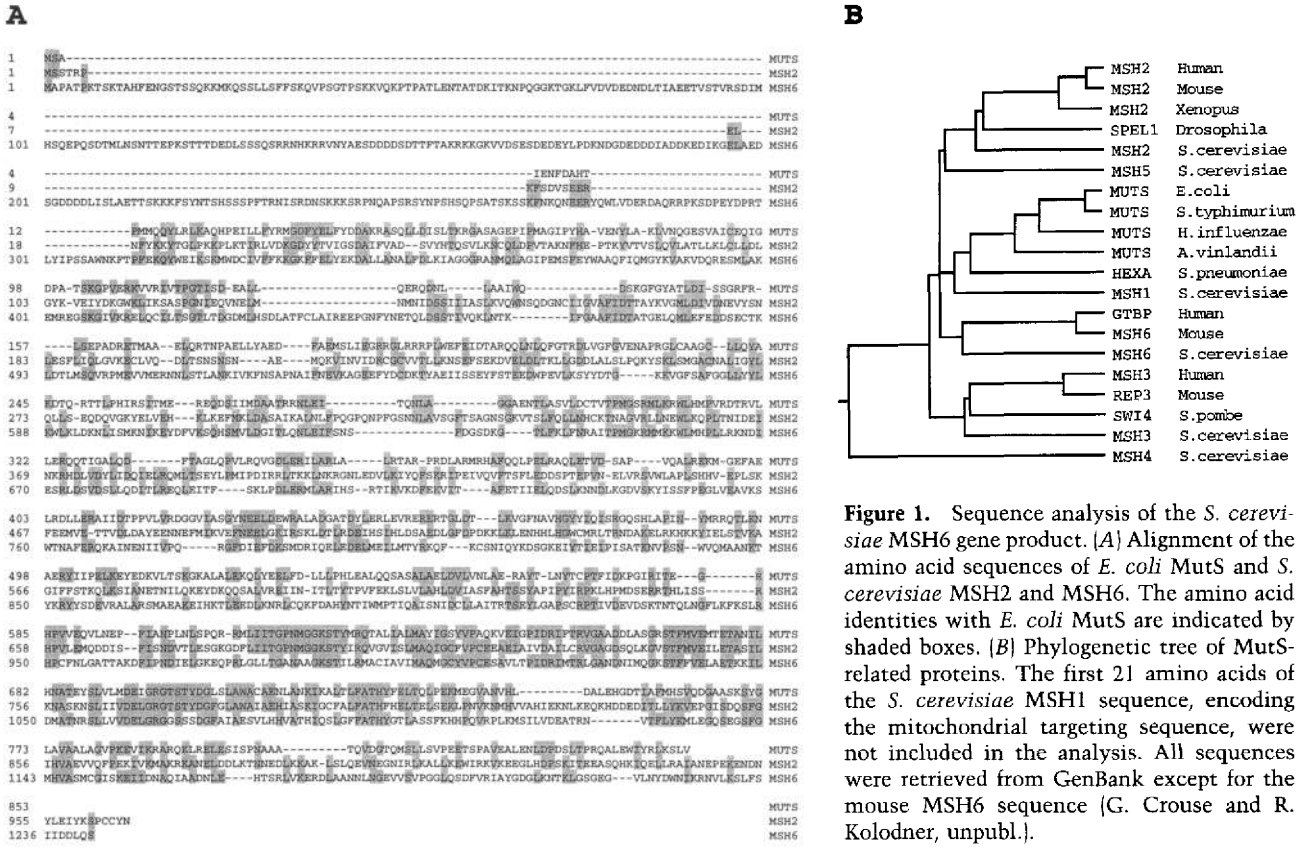

Figure 1. Sequence analysis of the *S. cerevisiae* MSH6 gene product. (*A*) Alignment of the amino acid sequences of *E. coli* MutS and *S. cerevisiae* MSH2 and MSH6. The amino acid identities with *E. coli* MutS are indicated by shaded boxes. (*B*) Phylogenetic tree of MutS-related proteins. The first 21 amino acids of the *S. cerevisiae* MSH1 sequence, encoding the mitochondrial targeting sequence, were not included in the analysis. All sequences were retrieved from GenBank except for the mouse MSH6 sequence (G. Crouse and R. Kolodner, unpubl.).

detected the production of canavanine-resistant mutants (Can^r). To further analyze this mutator phenotype, a series of isogenic strains was constructed containing the *hom3-10* and *lys2–Bgl* alleles (+1 and +4 base frameshift mutations, respectively) and either *msh6*, *msh2* or *msh6*, and *msh2* mutations. Patch tests (Fig. 2; data not shown) demonstrated that in all cases analyzed, the *msh6* mutation caused an increase in the rate of accumulation of Can^r mutations, but only a very small increase in reversion of *hom3-10* or *lys2–Bgl* (7 isolates analyzed) compared to that seen in a *msh2* mutant. This was in contrast to the *msh2* (13 isolates analyzed) and *msh2, msh6* (5 isolates analyzed) strains that had a similar increase in both the rate of accumulation of Can^r mutations and reversion of *hom3-10* and *lys2–Bgl*.

Fluctuation analysis (described in Materials and methods) demonstrated that the rate of accumulation of Can^r mutations was 18-fold higher in a *msh6* mutant compared with wild type; however, there was a very small increase in the rate of reversion of *hom3-10* and *lys2–Bgl* in a *msh6* mutant compared with wild-type strains (Table 1). This was in contrast to *msh2* mutations, which caused increases in the rate of accumulation of Can^r mutations and reversion of *hom3-10* and *lys2–Bgl* by 40-, 662- and 55-fold, respectively; compared with the wild-type control strain. Note that whereas the rate of reversion of *hom3-10* and *lys2–Bgl* observed in the *msh6* mutant was significantly higher than the wild-type rate, it was at best 1% of the rate of reversion of *hom3-10* and *lys2–Bgl* observed in *msh2* mutants. The rate of accumulation of mutations in the *msh2, msh6* strain was similar to that of the *msh2* strain, consistent with *MSH2* being epistatic to *MSH6*.

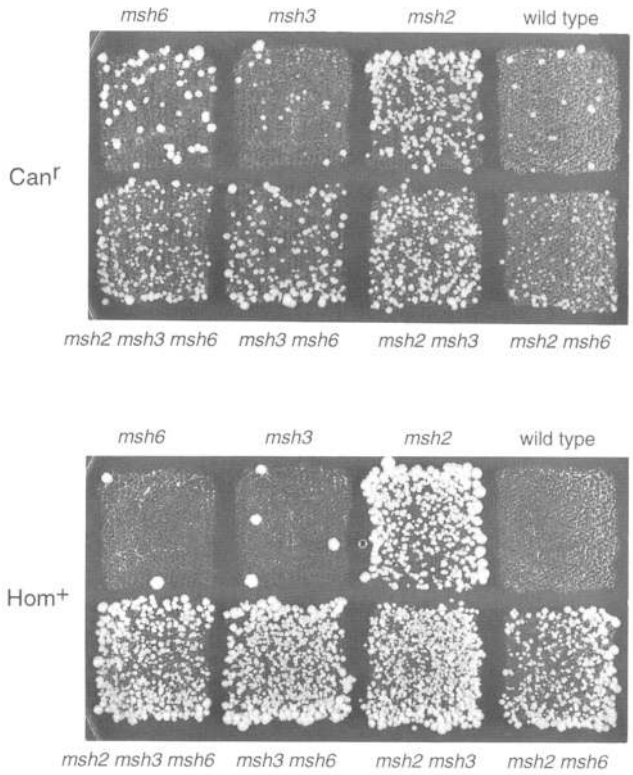

Figure 2. Qualitative analysis of the mutator phenotype of *S. cerevisiae* strains containing different combinations of mutations in *MSH2, MSH3* and *MSH6*. Patches of the indicated strains were made on a YPD plate that was incubated at 30°C for 2 days. This master plate was then replica-plated to one canavanine plate, one threonine dropout plate, and one lysine dropout plate (not shown) to detect the increased presence of Can^r mutants, Hom$^+$ revertants and Lys$^+$ revertants, which appeared as papillae after incubation of the plates at 30°C for 2 days.

Analysis of the spectrum of mutations that accumulate in msh2 *and* msh6 *mutants*

To gain insight into the repair events in which *MSH2* and *MSH6* participate, the sequence of the Can^r mutations arising in *msh2* and *msh6* mutants and the sequence of the Hom$^+$ and Lys$^+$ mutations arising in *msh2* mutants were determined. The sequences of only a small number of the Hom$^+$ and Lys$^+$ mutations arising in *msh6* mutants were determined because *hom3-10* and *lys2–Bgl* only revert at a low rate above background, making it difficult to isolate such mutations or perform a definitive analysis in this case.

To determine the sequence of the Hom$^+$ revertants, it was first necessary to determine the sequence of the *hom3-10* allele. The *hom3-10* allele present in several different *S. cerevisiae* strains (RKY2575 constructed in this laboratory by gene replacement using pK8; MW3069-15A and MW3070-6C constructed in the laboratory of S. Fogel and supplied by A. Jeyaprakash, University of Florida, Gainesville) and the *hom3-10* allele that had been rescued onto a plasmid were sequenced. Analysis of these sequence data demonstrated that *hom3-10* was a +1 frameshift mutation caused by the insertion of a single T in a run of 6 T's constituting nucleotides 646–651 of the wild-type gene (Fig. 3).

The most probable mechanism by which frameshift mutations such as *hom3-10* and *lys2–Bgl* revert is either through direct reversion to the wild-type allele or by mutation events resulting in the insertion/deletion of nucleotides between the relevant upstream or downstream stop codons and the original mutation such that the correct reading frame is restored. Analysis of 20 or more each Hom$^+$ and Lys$^+$ revertants arising in a *msh2* mutant showed that all reversion events involved the deletion of one nucleotide to restore the correct open reading frame. All of the deletion events were the deletion of a single nucleotide in short mononucleotide repeat sequences, similar to the prevalence of deletions seen during instability of dinucleotide repeat sequences in mismatch repair mutants (Strand et al. 1993). The observation that all of the Hom$^+$ revertants were caused by the deletion of a single T in a run of 7 T's suggests that the *hom3-10* reversion assay is the equivalent of the mononucleotide repeat instability assays used to study repeat instability in human tumor cells in some cases (Shibata et al. 1994; Papadopoulos et al. 1995). These data (Table 2; Fig. 3) support the idea that insertion/deletion mis-

Table 1. *Mutation rate analysis*

Genotype	Rate test		
	Can^r	Hom$^+$	Lys$^+$
Wild type	8.0×10^{-8}	1.5×10^{-8}	2.9×10^{-8}
	1.2×10^{-7} (1)	1.0×10^{-8} (1)	1.4×10^{-8} (1)
msh2	4.3×10^{-6}	5.2×10^{-6}	1.7×10^{-6}
	3.7×10^{-6} (40)	1.2×10^{-5} (662)	7.3×10^{-7} (55)
msh3	9.9×10^{-8}	7.4×10^{-8}	7.4×10^{-8}
	1.1×10^{-7} (1)	3.4×10^{-8} (4)	1.7×10^{-8} (2)
msh6	1.8×10^{-6}	1.0×10^{-7}	5.2×10^{-8}
	1.8×10^{-6} (18)	1.2×10^{-7} (8)	1.0×10^{-7} (3)
msh2 msh6	8.1×10^{-6}	5.2×10^{-6}	1.7×10^{-6}
	2.9×10^{-6} (55)	2.6×10^{-6} (300)	2.2×10^{-6} (91)
msh2 msh3	3.7×10^{-6}	6.7×10^{-6}	6.8×10^{-7}
	2.1×10^{-6} (29)	4.7×10^{-6} (438)	6.8×10^{-7} (31)
msh3 msh6	3.3×10^{-6}	6.6×10^{-6}	3.3×10^{-6}
	4.0×10^{-6} (37)	8.6×10^{-6} (585)	2.0×10^{-6} (123)
msh2 msh3 msh6	3.1×10^{-6}	6.0×10^{-6}	6.1×10^{-7}
	2.5×10^{-6} (28)	5.1×10^{-6} (431)	6.4×10^{-7} (29)

The data from two independent experiments are presented. The number in parenthesis is the fold induction relative to the wild-type value based on the average of the data from both experiments. The strains tested were RKY 2575 (wild type), RKY 2558 (*msh2*), RKY 2582 (*msh3*), RKY 2580 (*msh6*), RKY 2581 (*msh2 msh6*), RKY 2561 (*msh2 msh3*), RKY 2567 (*msh3 msh6*), and RKY 2571 (*msh2 msh3 msh6*).

pairs produced by DNA polymerase errors are not corrected in *msh2* mutants. The small number of Hom$^+$ and Lys$^+$ revertants we were able to obtain from *msh6* mutants were all −1 frameshift mutations of the type seen in *msh2* mutants (Table 2). The limited reversion of *hom3-10* and *lys2–Bgl* seen in *msh6* mutants (~1% of the rate seen in a *msh2* mutant) and the type of mutations obtained suggest that *msh6* mutants have at best a small defect in recognition of insertion/deletion mispairs, including 1-base insertion/deletion mispairs.

To gain further insight into *MSH2*- and *MSH6*-dependent repair, the Can^r mutations (any mutation inactivating the arginine permease gene) arising in *msh2* and *msh6* mutants were sequenced. This assay is particularly useful because unlike the *hom3-10* and *lys2–Bgl* reversion assays, the Can^r mutation assay is unbiased and can detect any type of inactivating mutation that can occur in the ~1.8-kb arginine permease gene. The data (Table 3) demonstrate that 86% of the Can^r mutations in the *msh6* mutant were single-base substitutions, whereas the Can^r mutations arising in the *msh2* mutant were primarily (85%) single-base insertion/deletion muta-

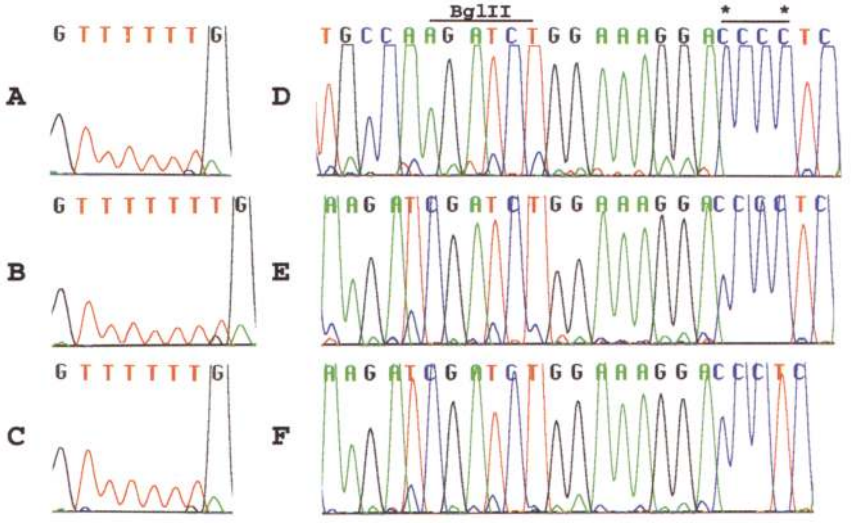

Figure 3. DNA sequence analysis of Hom$^+$ and Lys$^+$ revertants. Nucleotides 565–788 of the *HOM3* gene and nucleotides 270–583 of the *LYS2* gene were determined as described in Materials and methods; however, only the sequencing chromatogram of the coding strand of the region containing either the *hom3-10* or *lys2–Bgl* allele is shown. (*A*) Sequence chromatogram from a wild-type strain showing the 6T wild-type *HOM3* allele; (*B*) sequence chromatogram from a *hom3-10* mutant strain showing the 7T mutant allele; (*C*) sequence chromatogram from a Hom$^+$ revertant showing reversion to the 6T wild-type allele; (*D*) sequence chromatogram from a wild-type strain showing the wild-type *LYS2* allele; (*E*) sequence chromatogram from a *lys2–Bgl* mutant strain showing the GATC duplication caused by the *lys2–Bgl* allele; (*F*) sequence chromatogram from a Lys$^+$ revertant showing the 4 C's to 3 C's −1 frameshift, which restores the correct reading frame in the revertant. The site of the *Bgl*II site in the *LYS2* gene and the run of 4 C's in the *LYS2* gene where the −1 C deletion occurred in the Lys$^+$ revertant are indicated by overlining in *D*.

Table 2. *Mutation spectrum of Hom⁺ and Lys⁺ revertants*

		Hom⁺			Lys⁺	
Genotype		mutation	occurrence		mutation	occurrence
msh2	ΔT	$T_6 \rightarrow T_5$	22/22	ΔA	$A_6 \rightarrow A_5$	9/21
				ΔC	$C_4 \rightarrow C_3$	11/21
					$C_2 \rightarrow C_1$	1/21
msh6	ΔT	$T_6 \rightarrow T_5$	6/6	ΔA	$A_6 \rightarrow A_5$	1/4
				ΔT	$T_3 \rightarrow T_2$	3/4

The strains tested were RKY 2558 (*msh2*) and RKY 2580 (*msh6*). All of the Hom⁺ revertants involved the direct reversion of the 7T *hom3-10* allele to the 6T *HOM3* allele, whereas a variety of mutations at *LYS2* were observed. Only a summary of the mutations observed is presented. A detailed mutation spectrum is available on request.

tions (primarily deletions) in short mononucleotide repeat sequences. The accumulation of single-base substitution mutations in the *msh6* mutant (86% of an 18-fold increase in mutation rate) is, within the error of such measurements, equivalent to the rate of accumulation of such mutations in the *msh2* mutant (15% of a 40-fold increase in mutation rate). In contrast, the accumulation of insertion/deletion mutations in the *msh6* mutant accounts for at most a 2.5-fold increase in the rate of accumulation of mutations over background (14% of an 18-fold increase in mutation rate), which is consistent with the results obtained with the frameshift reversion assays. The sum of the mutational spectra data suggests that *MSH2* is required for a mismatch repair pathway that recognizes single-base mispairs and insertion/deletion mispairs, whereas *MSH6* is primarily required for recognition of single-base mispairs and at best plays only a small role in the repair of insertion/deletion mispairs including single-base insertion/deletion mispairs.

The pms3-1 *mutation is an allele of* MSH6

One of the original *pms* mutations, *pms3-1*, causes phenotypes that are similar to those caused by *msh6* mutations. *pms3-1* mutations cause an increased rate of accumulation of Can^r mutations but do not cause an increase in the rate of reversion of *hom3-10* (Williamson et al. 1985; Jeyaprakash et al. 1994). In addition, it has been shown that *pms3-1* mutations cause a complete defect in the repair of heteroduplex plasmid DNAs containing each of the eight possible single-base substitution mispairs, similar to that caused by mutations in *PMS1* and *PMS2* (*MLH1*). However, in contrast to mutations in *PMS1* and *PMS2* (the original *PMS2* gene is identical to *MLH1*; Jeyaprakash et al. 1996), *pms3-1* mutations do not cause a defect in repair of heteroduplex plasmid DNAs containing either a +A or a +T single-base insertion mispair (B. Kramer et al. 1989). To determine whether *pms3-1* is a allele of *MSH6*, we transformed a

Table 3. *Mutation spectrum of Can^r mutants*

		Insertion/deletion		Base change	
Genotype		mutation	occurrence	mutation	occurrence
msh2	ΔA	$A_6 \rightarrow A_5$	7/20	C → A	1/20
	ΔT	$T_6 \rightarrow T_5$	2/20	G → T	1/20
		$T_5 \rightarrow T_4$	2/20	T → G	1/20
		$T_4 \rightarrow T_3$	4/20		
		$T_3 \rightarrow T_2$	1/20		
	+T	$T_6 \rightarrow T_7$	1/20		
			17/20 (85%)		**(3/20 (15%)**
msh6	ΔT	$T_6 \rightarrow T_5$	1/21	C → A	1/21
		$T_2 \rightarrow T_1$	1/21	G → A	10/21
	ΔC	$C_3 \rightarrow C_2$	1/21	G → T	4/21
				T → C	2/21
				T → G	1/21
			3/21 (14%)		**18/21 (86%)**
msh3 msh6	ΔA	$A_6 \rightarrow A_5$	4/22	A → G	1/22
	ΔT	$T_6 \rightarrow T_5$	7/22	C → A	2/22
		$T_4 \rightarrow T_3$	2/22	G → T	2/22
	ΔG	$G_1 \rightarrow G_0$	1/22	G → A	1/22
	+T	$T_6 \rightarrow T_7$	1/22	T → C	1/22
			15/22 (68%)		**7/22 (32%)**

The strains tested were RKY 2558 (*msh2*), RKY 2580 (*msh6*), and RKY 2567 (*msh3 msh6*). Only a summary of the mutations observed is presented. A detailed mutation spectrum is available on request.

pms3-1 mutant strain with either a plasmid containing the wild-type *MSH6* gene or the cloning vector as a control and tested eight independent transformants each for complementaion of the *pms3-1* mutator phenotype using patch tests on canavanine plates as described in Fig. 2. In all cases, complete complementation was observed with the *MSH6* plasmid but not with the vector control, consistent with the idea that *pms3-1* is an allele of *MSH6*.

To confirm that *pms3-1* mutant strains contain a mutation in *MSH6*, the *MSH6* gene was amplified from both a *pms3-1* mutant and a wild-type parental strain and sequenced. One difference from the wild-type *MSH6* sequence was observed (Fig. 4). This change was a G → A change at nucleotide 1262 (codon 421), which results in a substitution of Asp for Gly, a significant amino acid change. This Gly is a highly conserved amino acid located in a conserved region of the known MutS homologs, except *S. cerevisiae* MSH4 and MSH5, which are highly divergent in this region (most amino acids in this region are not even present in MSH4 and MSH5). Gly-421 is perfectly conserved in a subset of MutS homologs: the MutS subfamily, the MSH2 subfamily, the MSH6 subfamily, and MSH1. In the MSH3 subfamily, this residue is either Gly, Ser, or Ala, the latter two amino acids being conservative substitutions. These data, combined with the observation that *MSH6* complements *pms3-1*, indicate that *pms3-1* is a missense mutation in *MSH6*. We propose that the *MSH6* gene continue be called

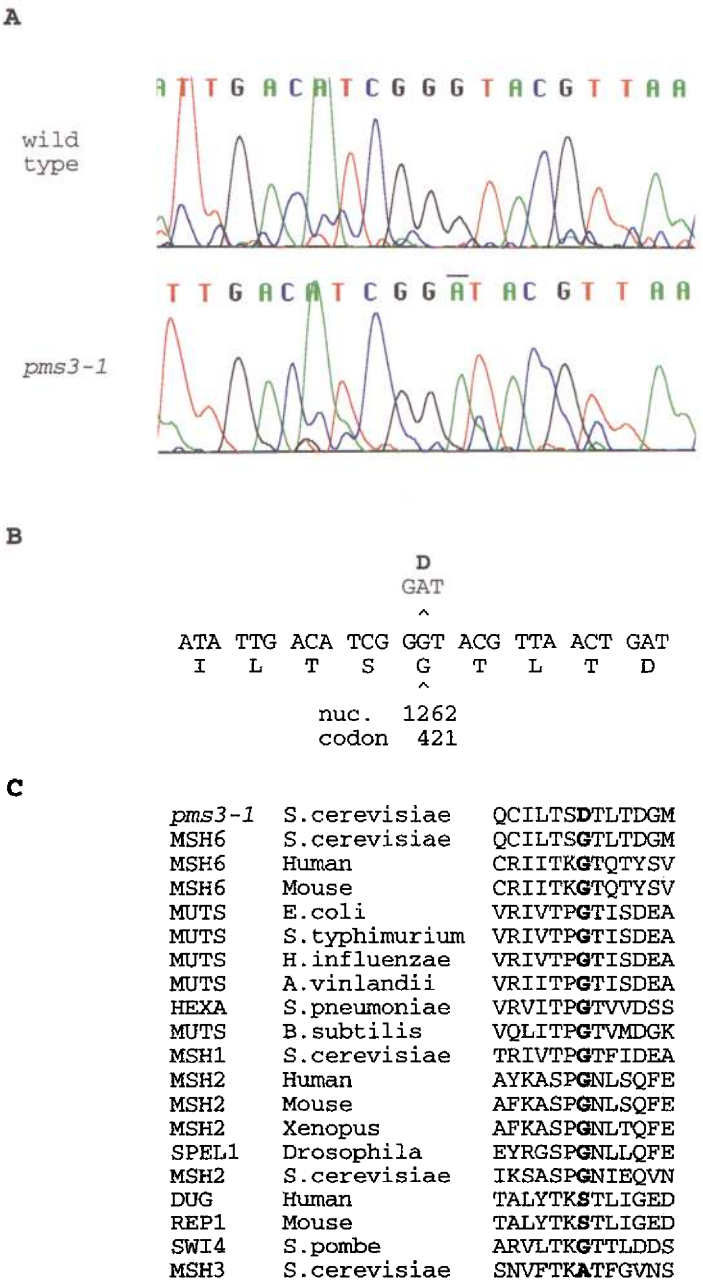

Figure 4. DNA sequence analysis of the *pms3-1* allele. The entire *MSH6* gene was sequenced from congenic wild-type and *pms3-1* strains as described in Materials and methods. (*A*) Sequence chromatogram of nucleotides 1252–1270 of the *MSH6* gene and the *pms3-1* allele. The G → A change at nucleotide 1262 is overlined. (*B*) DNA sequence of nucleotides 1249–1275 of the *MSH6* gene with the translated amino acid sequence listed below and the effect of the *pms3-1* mutation on the DNA and amino acid sequence indicated above. (*C*) Alignment of the relevant region of amino acid sequence from different MutS homologs and the *pms3-1* allele of *S. cerevisiae MSH6*. *S. cerevisiae* MSH4 and MSH5 are not shown as they are highly divergent in this region. Most amino acids in this region are not even present in MSH4 and MSH5. The conserved Gly-421 and equivalent residues in other MutS homologs are indicated in bold.

MSH6 because this designation provides information about the function of the gene; in keeping with this, *pms3-1* should be renamed *msh6-1*.

Analysis of the role of MSH3 *in mismatch repair*

The low rate of accumulation of insertion/deletion mutations in *msh6* mutants is reminiscent of *msh3* mutants, which show low but increased rates of reversion of *hom3-10* and *lys2–Bgl* but essentially no increased rate of accumulation of Can^r mutants (New et al. 1993; Alani et al. 1994). One explanation for the low rate of accumulation of insertion/deletion mutations in *msh6* and *msh3* single mutants is that there are two mismatch repair pathways: a *MSH2, MSH6* pathway, which recognizes single-base mispairs and insertion/deletion mispairs, and a *MSH2, MSH3* pathway, which only recognizes insertion/deletion mispairs. To test this possibility, a *msh3, msh6* double mutant was constructed and analyzed to determine the effect of this double mutation combination on the accumulation of mutations.

The results (Table 1; Fig. 2) demonstrated that the rate of accumulation of Can^r mutations and the rate of reversion of *hom3-10* and *lys2–Bgl* in the *msh3, msh6* double mutant (8 isolates analyzed) was increased synergistically in comparison with either the *msh3* or *msh6* single mutants (5 and 7 isolates analyzed, respectively) and was essentially indistinguishable from that observed in a *msh2* single mutant (13 isolates analyzed). Both the *msh2, msh3* double mutant strain (two isolates analyzed) and the *msh2, msh3, msh6* triple mutant strain (two isolates analyzed) had the same phenotype as the *msh2* single mutant, as assessed in both patch tests (Fig. 2) and quantitative rate tests (Table 1), suggesting that *MSH2* is epistatic to *MSH3* and *MSH6*. There are some small differences in mutation rates seen in the strains containing multiple combinations of *msh2, msh3* and *msh6* mutations relative to *msh2* mutant strains; however these differences are no more than about two-fold, which is the level of variation seen in these types of experiments.

Sequence analysis of the Can^r mutations that occurred in the *msh3, msh6* double mutant demonstrates that like the *msh2* single mutant, single-base insertion/deletion mutations (primarily deletions) in short mononucleotide repeat sequences predominate over single-base substitution mutations in the *msh3, msh6* double mutant (Table 3). The mutation spectrum of Can^r mutations in the *msh3* single mutant was not analyzed because the rate of accumulation of mutations in *msh3* mutants is essentially the same as in wild-type control strains. Within the error caused by the sample size used, the mutation spectrum in the *msh3, msh6* double mutant is essentially the same as in the *msh2* single mutant, both with regard to the preponderance of single-base insertion/deletion mutations and the type of insertion/deletion mutations seen. This result indicates that the synergistic effect of *msh3* and *msh6* mutations is primarily confined to the rate of accumulation of insertion/deletion mutations and that the rate of accumulation of single-base substitution mutations is similar to that observed in either *msh2* or *msh6* single mutants. These data are consistent with the idea that a combination of mutations in *MSH3* and *MSH6* inactivates mismatch repair in a way that is similar to that caused by mutations in *MSH2*. However, our data do not rule out the possibility that there are small differences in mutagenesis in the *msh3, msh6* double mutant compared with the *msh2* single mutant.

MSH2 interacts with MSH3 and MSH6

The observation that human MSH2 interacts with the human homolog of MSH6, GTBP/p160, suggests that MSH2 might interact with both MSH3 and MSH6. To test this possibility, MSH3, hexa-His-tagged MSH3, MSH6, hexa-His-tagged MSH6, MSH2, and 12CA5-epitope-tagged MSH2 (Alani et al. 1995) were transcribed and translated in vitro to determine whether MSH2 could interact with MSH3 or MSH6. The DNA templates used in these studies were produced by PCR and contained only the *MSH3*, hexa-His-tagged *MSH3*, *MSH6*, hexa-His-tagged *MSH6*, *MSH2*, and 12CA5 epitope-tagged *MSH2* coding sequences, as needed to ensure that only these proteins were synthesized. Control experiments verified that for each of these proteins, full-length protein could be synthesized under the in vitro transcription and translation conditions used.

To detect interactions between MSH2 and MSH6, different combinations of MSH6 or hexa-His-tagged MSH6 plus MSH2 or 12CA5-epitope-tagged MSH2 were cotranscribed and translated in the presence of [^{35}S]methionine. These proteins were then analyzed using a two-step procedure in which the proteins were first captured and eluted from Ni-beads and then immunoprecipitated with anti-12CA5 antibody (Fig. 5A). A 140-kD polypeptide the size of MSH6 and a 109-kD polypeptide the size of MSH2 were coimmunoprecipitated only when MSH6 contained the hexa-His tag and MSH2 contained the 12CA5 epitope. The recovery of this complex was dependent on the presence of the 12CA5 MSH2 epitope, the hexa-His MSH6 tag, the MSH6 coding region (Fig. 5A), and the MSH2 coding region (data not shown), indicating that the observed complex was caused by a specific interaction between MSH2 and MSH6. An identical series of experiments was also performed to determine whether MSH3 would interact with MSH2 except that the *MSH3* gene sequence was substituted for the *MSH6* gene sequence (data not shown). These experiments similarly demonstrated that a 120-kD polypeptide the size of MSH3 and a 109-kD polypeptide the size of MSH2 protein were coimmunoprecipitated only when MSH3 contained the hexa-His tag and MSH2 contained the 12CA5 epitope. The recovery of this complex was dependent on the presence of the 12CA5 MSH2 epitope, the hexa-His MSH3 tag, the MSH3 coding region, and the MSH2 coding region (data not shown), indicating that the observed complex was attributable to a specific interaction between MSH2 and MSH3. In these experiments, the MSH2–MSH3 and

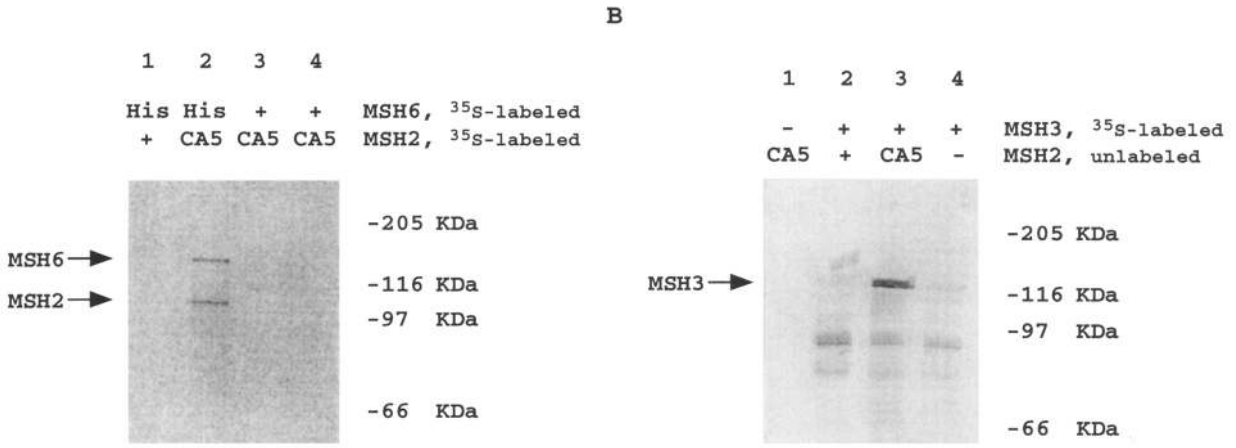

Figure 5. MSH2 protein interacts with MSH3 and MSH6. (*A*) Different combinations of pairs of MSH6, hexa-His-tagged MSH6, MSH2, and 12CA5-epitope-tagged MSH2 proteins and mock proteins (no template DNA added) were prepared by co-in vitro transcription–translation as indicated in the presence of [^{35}S]methionine and analyzed by capture on Ni-beads followed by immunoprecipitation with anti-12CA5 monoclonal antibody in the presence of 1% Triton X-100 and 0.5 M NaCl as described in Materials and methods. An aliquot of each reaction was analyzed prior to processing with Ni-beads and 12CA5 antibody to ensure that all of the proteins had been synthesized (data not shown). (Lane *1*) Hexa-His-tagged MSH6 + MSH2; (lane *2*) hexa-His-tagged MSH6 + 12CA5 epitope-tagged MSH2; (lane *3*) MSH6 + 12CA5 epitope-tagged MSH2; (lane *4*) 12CA5 epitope-tagged MSH2 with no *MSH6* template. The position where protein standards migrated on the same gel is indicated as are the positions where MSH2 and MSH6 are expected to migrate. (*B*) MSH3 protein and mock proteins (no template DNA added) were prepared by in vitro transcription–translation as indicated in the presence of [^{35}S]methionine. These proteins were mixed with unlabeled MSH2 protein or 12CA5-epitope-tagged MSH2 protein prepared by in vitro transcription–translation as indicated and analyzed by immunoprecipitation with anti-12CA5 monoclonal antibody in the presence of 1% Triton X-100 and 0.5 M NaCl as described in Materials and methods. An aliquot of each reaction was analyzed before processing with 12CA5 antibody to ensure that MSH3 protein had been synthesized in all reactions (data not shown). In addition, the MSH2 templates were analyzed by in vitro transcription–translation in parallel reactions in the same experiment to ensure that they directed the synthesis of MSH2 and 12CA5-epitope-tagged MSH2 (data not shown). (Lane *1*) 12CA5 epitope-tagged MSH2 with no *MSH3* template; (lane *2*) MSH3 + 12CA5 epitope-tagged MSH2; (lane *3*) MSH3 + MSH2; (lane *4*) MSH3 with no *MSH2* template. The position where protein standards migrated on the same gel is indicated, as is the position where MSH3 is expected to migrate. For templates added to in vitro transcription–translation reactions: (−) no template; (+) wild-type template; (His) hexa-His-tagged template; (CA5) 12CA5 epitope-tagged template.

MSH2–MSH6 complexes could be quantitatively recovered by immunoprecipitation in the presence of 1% Triton X-100 and 0.5 M NaCl, indicating that they were the result of a strong interaction between the proteins.

A second series of experiments was performed in which individual proteins were separately transcribed and translated in vitro and then mixed together to allow complex formation to occur. These experiments (Fig. 5B) demonstrated that a 120-kD polypeptide, which is the predicted size of MSH3, could be immunoprecipitated by anti-12CA5 antibody if translated ^{35}S-labeled MSH3 was mixed with epitope-tagged MSH2. The 120-kD MSH3 polypeptide was not immunoprecipitated if the *MSH3* gene was not included in the transcription–translation mixes or if the translated MSH2 did not contain the 12CA5 epitope. These experiments indicated that the 120-kD MSH3 polypeptide was immunoprecipitated only in the presence of 12CA5 epitope-tagged MSH2, indicating a specific interaction between MSH3 and MSH2. An identical series of experiments was also performed to determine whether MSH6 would interact with MSH2, except that the *MSH6* gene was substituted for the *MSH3* gene (data not shown). These experiments similarly demonstrated that the 140-kD polypeptide encoded by the *MSH6* gene specifically interacted with the MSH2 protein and could be immunoprecipitated through a specific interaction with MSH2. In these experiments, the MSH2–MSH3 and MSH2–MSH6 complexes could be quantitatively recovered by immunoprecipitation in the presence of 1% Triton X-100 and 0.5 M NaCl, indicating that they were the result of a strong interaction between the proteins.

Discussion

In this communication we describe a sixth *S. cerevisiae MSH* gene, *MSH6*. The MSH6 protein is related most closely to GTBP/p160, a protein identified because it interacts with human MSH2 and thus appears to be a second subunit of a human mispair recognition complex (Drummond et al. 1995; Palombo et al. 1995). Mutations in *MSH6* cause a partial mutator phenotype consistent with a defect in recognition of single-base mispairs similar to that observed in a *msh2* mutant, but only a small defect (~1%) in the recognition of insertion/deletion mispairs compared with that observed in *msh2* mutants. The prior demonstration that *pms3-1* mutations cause a direct defect in the repair of single-base substitution

mispairs and not single-base insertion mispairs (B. Kramer et al. 1989), combined with the observation presented here that *pms3-1* mutations are alleles of *MSH6*, confirm that *msh6* mutations cause a specific defect in the repair of single-base substitution mispairs but not single-base insertion mispairs. In contrast, *msh2* mutations cause defects that are consistent with a defect in recognition of both single-base and insertion/deletion mispairs during mismatch repair. The analysis of *msh3* mutations presented here confirms previously published results that *msh3* mutations cause only limited defects in mismatch repair (New et al. 1993; Alani et al. 1994). Surprisingly, *msh3, msh6* double mutant strains had essentially the same mutator phenotype and mutation spectrum as *msh2* mutant strains. The ~100-fold synergistic effect of *msh3* and *msh6* mutations on the rate of accumulation of mutations is confined to the accumulation of insertion/deletion mutations, whereas the accumulation of single-base substitution mutations is *msh6* dependent and *msh3* independent. Epistasis analysis of *MSH2, MSH3* and *MSH6* is consistent with the idea that *MSH3* and *MSH6* encode redundant functions that act in *MSH2*-dependent mismatch repair of insertion/deletion mispairs, whereas *MSH6* appears to also be required for *MSH2*-dependent mismatch repair of single-base substitution mispairs.

Fig. 6 illustrates a model that is consistent with the results presented above. Based on the observations that human GTBP/p160 (MSH6) forms a heterodimer with MSH2, which recognizes mispaired bases (Drummond et al. 1995; Palombo et al. 1995), and that *S. cerevisiae* MSH2 forms complexes with both MSH3 and MSH6, we propose that there are two mispair recognition complexes: an MSH2–MSH6 complex that recognizes both single-base mispairs and insertion/deletion mispairs, and a MSH2–MSH3 complex that recognizes insertion/deletion mispairs and does not recognize single-base mispairs or has only very low affinity for them. Given that MSH2 can recognize mispaired bases by itself (Fishel et al. 1994; Alani et al. 1995), MSH3 and MSH6 could either modify the specificity of MSH2 or could participate directly in mismatch recognition. The proposed relative affinity of each complex for different mispairs and the redundancy of *MSH3* and *MSH6* with regard to recognition of insertion/deletion mispairs provides an explanation for the following observations: (1) the strong mutator phenotype caused by *msh2* mutations; (2) the accumulation of single-base substitution mutations in *msh6* mutants; (3) the lack of effect of *msh3* and *msh6* mutations on accumulation of insertion/deletion mutations; (4) the observation that *msh6* (*pms3-1*) mutations cause a direct defect in the repair of single-base substitution mispairs but not single-base insertion mispairs (B. Kramer et al. 1989); and (5) the synergistic effect of *msh3* and *msh6* mutations on the accumulation of insertion/deletion mutations. Whereas the proposed model is consistent with both the genetic data and the protein–protein interaction data presented here, a complete test of this model will require purification of each complex and analysis of its mispair binding properties, which is in progress. Furthermore, whereas our data are consistent with the idea that MSH2–MSH3 and MSH2–MSH6 complexes direct the majority of mismatch repair, it remains possible that any one of these proteins can form complexes with itself and that such complexes can direct a limited amount of mismatch repair. This may explain how MSH2 recognizes mispaired bases by itself.

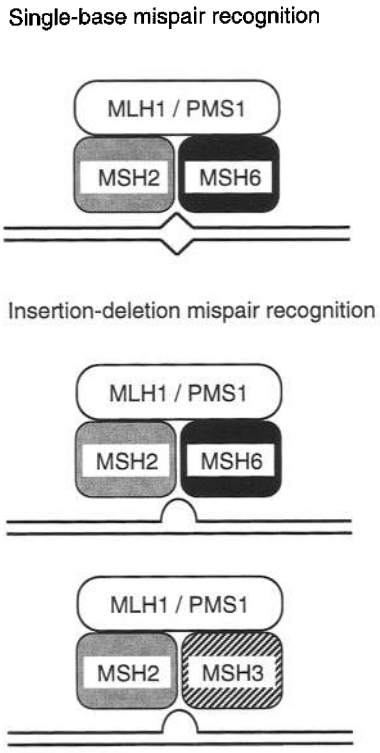

Figure 6. Model for mismatch recognition in *S. cerevisiae*. The various postulated complexes between MSH2 and either MSH3 or MSH6 are illustrated interacting with either a single-base substitution mispair or an insertion/deletion mispair; exactly which of the proteins in these complexes, MSH2, MSH3, or MSH6 actually interacts with the mispaired base is not known. Also indicated is the previously described MLH1-PMS1 complex which interacts with the mispair recognition complex (Prolla et al. 1994). The *S. cerevisiae* protein names are given as primary names; the human protein names are the same except for PMS1, which is called PMS2 in humans, and MSH6, which has been called GTBP or p160 in humans.

In human tumor cell lines *gtbp* mutations cause a strong in vitro defect on repair of single-base substitution and single-base insertion/deletion mispairs and a variable partial defect in repair of larger insertion/deletion mispairs (Drummond et al. 1995). *GTBP* mutant human tumor cell lines have been reported to have microsatellite instability in vivo, at both mononucleotide and dinucleotide repeat loci, although apparently at lower rates than in tumor cell lines having mutations in *hMSH2* or *hMLH1* (Parsons et al. 1993; Bhattacharyya et al. 1994; Shibata et al. 1994; Umar et al. 1994; Papadopoulos et al. 1995). Our results with *msh6* mutants most closely resemble the results of microsatellite instability

analysis of *gtbp* mutant human tumor cell lines (Shibata et al. 1994; Papadopoulos et al. 1995). We do not understand the basis for the differences in results obtained with in vivo and in vitro measurements of the effect of *msh6/gtbp* mutations. It is possible these differences could be due to methodological differences, possible instability of selected proteins in mutant cells (Drummond et al. 1995) or the interaction between mismatch repair and DNA replication that occurs in vivo but not in vitro.

Mutations in *GTBP* (*MSH6*) have not been found in HNPCC families and have only been found in a small proportion of tumor cell lines (Papadopoulos et al. 1995). To our knowledge, no systematic search has been made for mutations in *hMSH3* (*DUG* and *MRP1* are other names for human *MSH3*) in HNPCC families. Such mutations must be rare in microsatellite unstable, mismatch repair-defective human tumor cell lines since the majority of such cell lines can be explained by the presence of either *msh2* or *mlh1* mutations (Boyer et al. 1995). Our results have important implications for the analysis of mismatch repair defective mutations and their association with cancer susceptibility. First, the redundancy of *MSH3* and *MSH6* compared with the apparently universal requirement for *MSH2* in mismatch repair provides an explanation for the high prevalence of *msh2* mutations in HNPCC families and human tumors (Fishel et al. 1993; Leach et al. 1993; Kolodner et al. 1994; Liu et al. 1994; Nystrom-Lahti et al. 1994; Borresen et al. 1995; Boyer et al. 1995). This is because independent mutations in both *MSH3* and *MSH6*, which seem unlikely, would be required to produce the same mismatch repair defect as that caused by mutations in *MSH2*. It is also possible that the lack of another entirely *MSH2*-dependent process rather than the loss of mismatch repair is the underlying cause of cancer susceptibility. Second, by selecting for tumors and syndromes (HNPCC) associated with high degrees of microsatellite instability (Aaltonen et al. 1993; Ionov et al. 1993; Peltomaki et al. 1993a,b; Bhattacharyya et al. 1994; Honchel et al. 1994; Orth et al. 1994; Shibata et al. 1994; Eshleman and Markowitz 1995), one may select against cancers caused by *msh6* or *msh3* mutations. In contrast, one might expect to find *msh6* mutations associated with tumors that have increased rates of accumulating single-base substitution mutations but have little if any microsatellite instability (Eschelman et al. 1995). By analogy, one might only expect to find *msh3* mutations associated with cancers showing low level microsatellite instability but lacking other mutator phenotypes. Third, it is possible that the relatively low mutator phenotype caused by *msh3* or *msh6* mutations compared with *msh2* mutations is insufficient to cause cancer initiation or progression, or that such mutations have lower penetrance than *msh2* mutations. Finally, the mutational spectra presented here suggest that in human tumor cells having complete inactivation of *MSH2*-dependent mismatch repair, the most likely mutations to occur within gene coding sequences are frameshift mutations within short mononucleotide repeat sequences which can be quite prevalent within coding sequences.

Materials and methods

Strains, plasmids and media

All of the *S. cerevisiae* strains used in this study for the analysis of mutations in *MSH2, MSH3,* and *MSH6* were isogenic strains derived from a MGD strain provided by A. Nicolas (Rocco et al. 1992) and are listed in Table 4. The wild-type and *pms3-1* mutant strains used to analyze the *pms3-1* mutation were MW3070-6C and MW2049-24C, respectively, and were kindly provided by A. Jeyaprakash (Jeyaprakash et al. 1994). Disruption mutations in *MSH2, MSH3* and *MSH6* as well as the *hom3-10* and *lys2–Bgl* mutations were introduced by standard lithium acetate transformation based gene disruption techniques and, in some cases, by crossing mutant derivatives to isogenic derivatives of MGD. The presence of mutations in *MSH2, MSH3* and *MSH6* was always verified using PCR amplification of the mutant and wild-type alleles, whereas the presence of *hom3-10* and *lys2–Bgl* was verified by PCR amplification followed by DNA sequence analysis (see below). Derivatives of strains in which the *URA3* gene had been excised by recombination between *hisG* repeats were selected on minimal dropout plates containing 5-FOA.

The *MSH6* gene (S51246, YD8557.04c) was disrupted using a PCR-based method to generate a DNA fragment consisting of the *URA3* gene flanked by DNA from the 5′ and 3′ ends of the *MSH6* gene. DNA from the 5′ end of *MSH6* was amplified with

Table 4. S. cerevisiae *strains used in this study*

Strain	Genotype
RKY 2583	*MAT***a**/α, *ade2/ADE2, ura3-52/ura3-52, trpl-289/trp1-289, leu2-3,112/leu2-3,112, HIS3/his3Δ1, CYH2/cyh2*
RKY 2558	*MAT***a**, *ade2 ura3-52, leu2-3,112, trp1-289, his3Δ1, lys2–Bgl, hom3-10, msh2::hisG*
RKY 2569	*MAT***a** *ADE2, ura3-52, leu2-3,112, trp1-289, his3Δ1, lys2–Bgl, hom3-10, msh2::hisG, msh3::hisG–URA3–hisG*
RKY 2567	*MAT***a**, *ade2, ura3-52, leu2-3,112, trp1-289, his3Δ1, lys2–Bgl, hom3-10, msh3::hisG–URA3–hisG, msh6::URA3*
RKY 2571	*MAT***a**, *ade2, ura3-52, leu2-3,112, trp1-289, his3Δ1, lys2–Bgl, hom3-10, msh2::hisG, msh3::hisG–URA3–hisG, msh6::URA3*
RKY 2575	*MAT***a**, *ade2, ura3-52, leu2-3,112, trp1-289, his3Δ1, lys2–Bgl, hom3-10*
RKY 2580	*MAT***a**, *ade2, ura3-52, leu2-3,112, trp1-289, his3Δ1, lys2–Bgl, hom3-10, msh6::URA3*
RKY 2581	*MAT***a**, *ade2, ura3-52, leu2-3,112,trp1-289, his3Δ1, lys2–Bgl, hom3-10, msh2::hisG, msh6::URA3*
RKY 2582	*MAT***a**, *ade2, ura3-52, leu2-3,112, trp1-289, his3Δ1, lys2–Bgl, hom3-10, msh3::hisG–URA3–hisG*
RKY 2584	*MAT***a**, *ade2, ura3-52, leu2-3,112, trp1-289, his3Δ1, lys2–Bgl, hom3-10, msh3::hisG*
RKY 2585	*MAT***a**, *ade2, ura3-52, leu2-3,112, trp1-289, his3Δ1, lys2–Bgl, hom3-10, msh3::hisG, msh6::URA3*

primers 21355 (5′-GGTTCCGCGTGGATCCATGGCCCC-AGCTACCCCTAAAACTTC) and 21737 (5′-CGATGATAAG-CTGTCAAACATGAGAATTCGAGATTGGGAAGATGATA-AAATCCTC), and the 3′ end of *MSH6* was amplified with the primers 21740 (5′-GTTCCAATCATAGTTCAAGAC) and 21738 (5′-CATGGCGACCACACCCGTCCTGTGGATCCGA-GGTGGACTCGAAAACGAATACTC). The 5′ ends of primers 21737 and 21738 contain sequence that includes the *Bam*HI and *Eco*RI sites flanking the *URA3* gene on the plasmid YEp24 . The 3.3-kb disruption fragment was created by amplifying the 0.4-kb 5′ MSH6 and the 0.9-kb 3′ MSH6 fragments together with a *Bam*HI/*Eco*RI digest of YEp24 using the primers 21355 and 21740. This yielded a *MSH6* DNA fragment containing 0.4 kb of 5′ homology and 0.9 kb of 3′ homology in which the DNA sequence encoding amino acids 132–929 of MSH6 had been substituted by *URA3*. The disruption fragment was then transformed into the diploid MGD strain RKY2583, and disruptants were selected on URA dropout plates. Haploid *msh6::URA3* strains were obtained by sporulation. This *msh6::URA3* disruption was often moved into other strains by amplifying the *msh6::URA3* chromosomal region by long-range PCR (Barnes 1994; see also DNA sequencing, below) using primers 22604 (5′-CATCGGTTAAGCTTCTCGAGTCGACAAGAAATGGA-AAATACTAAATTAGCTG) and 22605 (5′-CATCTGTTC-CCGGGATCCCTGATTTTTTGCAGCATGCTCTCC) and then using the amplification product to transform strains to Ura$^+$.

The *MSH3::hisG–URA3–hisG* disruption plasmid, pEN33 has been described previously (Alani et al. 1994). The *MSH2::hisG–URA3–hisG* disruption plasmid, pRDK351, is a similar plasmid constructed in this laboratory by Eric Alani. The *lys2–Bgl* disruption plasmid pSR125 was obtained from S. Jinks-Robertson (Steele and Jinks-Robertson 1992). The plasmid pK8, which contains the *hom3-10* allele cloned into YIp5, was constructed in this laboratory by Brett Satterberg. The plasmids pEN11 and pEN43, which contain the wild-type and 12CA5 epitope-tagged *MSH2* gene, respectively, have been described previously (Alani et al. 1995). The plasmids pRDK377 and pEN28, which contain the wild-type *MSH6* and *MSH3* genes, respectively, will be described elsewhere. All of these plasmids were maintained in *recA E. coli* strains.

YPD liquid media, YPD plates, 5-FOA plates, minimal dropout plates and sporulation medium used for propagation and analysis of *S. cerevisiae* strains were prepared as described previously (Reenan and Kolodner 1992a; Alani et al. 1994). Can^r resistant mutants were selected on arginine dropout plates containing 60 mg/liter of canavanine as described previously (Reenan and Kolodner 1992a; Alani et al. 1994). Hom$^+$ revertants were selected for on minimal dropout plates lacking threonine and Lys$^+$ revertants were selected for on minimal dropout plates lacking lysine.

Genetic analysis

The rate of accumulation of Can^r mutants, Hom$^+$ revertants, and Lys$^+$ revertants in cell populations was determined by fluctuation analysis using the method of the median (Lea and Coulson 1948) as described previously (Reenan and Kolodner 1992a; Alani et al. 1994). In these fluctuation tests, five independent cultures were analyzed for each experiment and each culture was grown to a sufficient cell density so that mutant cells were obtained from each culture. Each fluctuation test was repeated independently at least two times. Independent Can^r mutants, Hom$^+$ revertants, and Lys$^+$ revertants were isolated by first streaking the strain of interest to single colonies on YPD plates. Then, single colonies, 1-mm in diameter, were patched onto plates containing canavanine or dropout plates lacking either threonine or lysine, and a single mutant or revertant per patch was purified by streaking to single colonies on selective media. Under these conditions, we did not obtain Can^r mutants, Hom$^+$ revertants, or Lys$^+$ revertants from *msh3* mutants or wild-type strains because of the low mutation rates in these strains.

DNA sequencing

All DNA sequencing was performed using an Applied Biosystems 373A DNA sequencer using *Taq* DNA polymerase and Dye Terminators according to protocols supplied by the manufacturer essentially as described previously (Fishel et al. 1993; Kolodner et al. 1994, 1995). Sequencing chromatograms were analyzed using the Sequencher program (Gene Codes Corp., Ann Arbor, MI) and all sequence comparisons, alignments, and phylogenetic trees were generated using DNAStar software (DNAStar, Inc., Madison, WI). PCR primers for preparation of sequencing templates and sequencing primers were designed using the Oligo 4.0-S program (National Biosciences, Inc., Plymouth, MN) and were synthesized using standard solid-phase cyanoethyl phosphoramidite chemistry.

To identify the *hom3-10* mutation, pK8 DNA containing the cloned *hom3-10* allele was prepared using Plasmid Maxi kits obtained from Qiagen Inc. (Chatsworth, CA). The entire *HOM3* gene was then sequenced using the following primers: 21514 (5′-TAACAGTGCTCTACTCATTG), 21514 (5′-TAACAGT-GCTCTACTCATTG), 22181 (5′-CAACTTTTTACTCTACT-GTGG), 22184 (5′-TGTTGTGATTTGGCTTCGC), 22185 (5′-CTGCTTTATGTAATGACCG), 22186 (5′-AATCTACTCCA-CCACATCC), 22187 (5′-AATGCTGATGAACTACAAG), 20949 (5′-CATTAAAGTGAAGAAGAAAGG), 22188 (5′-CCAACTA-ATGAAACAATAG), and 22189 (5′-AAAGTGAAGAAGAA-AGGTGG). To confirm the sequence of the *hom3-10* allele, nucleotides 565–788 of the *HOM3* gene were amplified by PCR from several *HOM3* and *hom3-10* strains and the resulting PCR product was sequenced as described below.

To identify the mutations causing reversion of either *hom3-10* or *lys2–Bgl*, chromosomal DNA preparations were made by preparing glass bead lysates of cells harvested from a single colony using a method developed by D. Tishkoff in this laboratory. In the case of Hom$^+$ revertants, nucleotides 565–788 of the *HOM3* gene were amplified by PCR using primers 22392 (5′-CTTTCCTGGTTCAAGCATTG) and 22401 (5′-GGATCAG-CAGTAAATATACC). In the case of Lys$^+$ revertants, nucleotides 270–583 of the *LYS2* gene were amplified by PCR using primers 22428 (5′-CCAACGTGGTCATTTAATGAG) and 22429 (5′-GTAAATTGGTCCGCAACAATGG). PCR was performed in 25- to 100-μl reactions containing 20 mM Tris (pH 8.55), 16 mM ammonium sulfate, 2.5 mM $MgCl_2$, 150 μg/ml of BSA, 50 mM each of the four dNTPs, 0.2 mM of each primer, 0.5 units of Klentaq1 DNA polymerase (Ab Peptides, St. Louis, MO)/0.08 units of *Pfu* DNA polymerase (Stratagene, La Jolla, CA), and ~20 ng of genomic DNA (for 25 μl of PCR reaction). PCR was performed for one cycle of 95°C for 5 min and one cycle of 80°C for 5 min at which point the DNA polymerases were added followed by 27–30 cycles of 94°C for 15 sec, 55°C for 30 sec, 68°C for 60 sec, and one cycle of 72°C for 7 min. The resulting PCR products were purified using Qiagen QIAquick Spin PCR purification kits. The *HOM3* fragment was then sequenced with primer 22392 and the resulting *LYS2* fragment was sequenced with primer 22428.

To identify Can^r mutations, chromosomal DNA preparations were made using a minor modification of a Yeast Mini Prep method described previously (Sherman et al. 1986). The arginine permease gene was then amplified by PCR using primers

22413 (5′-CTTAACTCCTGTAAAAAC) and 22414 (5′-GAAATGGCGTGGGAATGTG). PCR was performed in 50- to 100-μl reactions, and the reaction products purified essentially as described above for the analysis for the *HOM3* and *LYS2* DNA fragments, except that the 68°C extension step in each PCR cycle was for 3 min instead of 30 sec. The PCR product was then sequenced with primers 22415 (5′-TATTGGTATGATTGCCCTTG), 22427 (5′-GAGTTCTGGGTCGCTTCCATC), 22412 (5′-CAATCTACTTCCTACGTTTC), 22414 (5′-GAAATGGCGTGGGAATGTG), and 22629 (5′-GAATATGCCAAAGAACCC).

To identify the *pms3-1* mutation, the *MSH6* gene was amplified by PCR from strains MW3070-6C (wild type) and MW2049-24C (*pms3-1* mutant) using primers 22604 (5′-CATCGGTTAAGCTTCTCGAGTCGACAAGAAATGGAAAATACTAAATTAGCTG) and 22605 (5′-CATCTGTTCCCGGGATCCCTGATTTTTTGCAGCATGCTCTCC) essentially as described above for the arginine permease gene. The resulting PCR fragment was then purified as described above for the analysis for the *HOM3* and *LYS2* DNA and sequenced using primers 23234 (5′-GGCCCCAGCTACCCCTAAAAC), 23236 (5′-CTTTTGAGAAGATGTGGAG), 23237 (5′-GGAGTGACATAATGCA-TTCTCAAG), 23312 (5′-GGAGAATTGGCAGAAGATAG), 23313 (5′-GAGTACGATCCAACAACACTG), 23314 (5′-GTCAATGTTGGCTAAAGAAATGAG), 23315 (5′-GTCGCAAGTAAGACCTATGGAAG), 23316 (5′-GGATTATTGTATTATTTTGAAGTGG), 23317 (5′-GCAGGCTCGATAGTGTTGAC), 23318 (5′-CCACAAAGGGGATTTGACATAG), 23319 (5′-CGTTAGAGGAGGACCTAAAAAATAG), 23320 (5′-GATTAGGATTGTTAACGGGTG), 23321 (5′-GCAGAAAGTGTGCTACATCATGTC), and 23322 (5′-GAATGGTGAAGTTGTCTCTGTG).

Protein analysis

DNA templates containing the T7 RNA polymerase promoter linked to the coding sequence of *MSH2*, 12CA5 epitope-tagged *MSH2*, *MSH3*, and *MSH6* for in vitro transcription and translation were prepared by PCR amplification. PCR reactions were performed essentially as described above for the analysis of Hom^+ and Lys^+ revertants and contained 100 ng of pEN11 DNA (*MSH2*), pEN43 DNA (12CA5 epitope-tagged *MSH2*), pEN28 DNA (*MSH3*), or pRDK377 DNA (*MSH6*) as template as required. The primers used for amplification of *MSH2* and 12CA5 epitope-tagged *MSH2* were 5′-MSH2–23587 (5′-GGATCCTAATACGACTCACTATAGGGAGACCACCatgtcctccactaggccagagc) and 3′-MSH2–23686 (5′-ctatcgattctcacttaagatgtcgttg). The primers used for amplification of *MSH3* were 5′-MSH3–23597 (5′-GGATCCTAATACGACTCACTATAGGGAGACCACCatggtgataggtaatgaacctaaactgg) and 3′-MSH3–23586 (5′-ggaacaattcaaaaacgagaaagtg). The primer 5′ hexa-His-tagged MSH3 23585 (5′-GGATCCTAATACGACTCACTATAGGGAGACCACCATGCATCATCATCATCATCATgtgataggtaatgaacctaaactgg) was substituted for primer 23597 for synthesis of hexa-His-tagged *MSH3*. And the primers used for amplification of *MSH6* were 5′-MSH6–23582 (5′-GGATCCTAATACGACTCACTATAGGGAGACCACCatggccccagctaccccctaaaacttc) and 3′-MSH6–23584 (5′-gcctgttctgaatccttttttcaacg). The primer 5′ hexa-His-tagged MSH6–23583 (5′-GGATCCTAATACGACTCACTATAGGGAGACCACCATGCATCATCATCATCATCATgccccagctaccccctaaaacttc) was substituted for primer 23592 for synthesis of hexa-His-tagged *MSH6*. In all cases uppercase type indicates the sequences containing the T7 promoter and lowercase type indicates the gene sequence. These DNA templates were then transcribed and translated in vitro in 50-μl volumes containing 400 ng of each required template DNA using TNT kits from Promega (Madison, WI) exactly as described by the manufacturer with or without added ^{35}S-labeled methionine (Amersham, Arlington Heights, IL) as required.

In experiments where the DNA templates were transcribed and translated individually, the resulting reaction mixtures were mixed and incubated on ice for 1 hr to allow proteins to interact. The proteins were then analyzed by immunoprecipitation in the presence of 1% Triton X-100 and 0.5 M NaCl with anti-12CA5 monoclonal antibody (Berkeley Antibodies, Richmond, CA) exactly as described previously (Alani et al. 1995) except that the resulting gels were analyzed by either autoradiography or PhosphorImager analysis (Molecular Dynamics, Sunnyvale, CA).

In some experiments, pairs of DNA templates were transcribed and translated together in the presence of [^{35}S]methionine. The reaction mixtures were placed on ice, and 50 μl of 2× Ni binding buffer [1 mM imidazole, 1 M NaCl, 2% Triton X-100, 50 mM Tris-Cl (pH 7.6), 2 mM EDTA, 5 mM 2-mercaptoethanol, 2 mM PMSF] was added to each 50 μl of reaction mixture followed by the addition of 20 μl of Ni–NTA–agarose beads (Qiagen, Chatsworth, CA; as a 50% suspension in 1× Ni binding buffer). After incubation on ice for 1 hr, the Ni-beads were collected by centrifugation in a microcentrifuge, washed four times with 150 μl of Ni binding buffer and the proteins were then eluted by addition of 100 μl of Ni elution buffer [500 mM imidazole, 0.5 M NaCl, 1% Triton X-100, 25 mM Tris-Cl (pH 7.6), 2 mM EDTA, 5 mM 2-mercaptoethanol, 1 mM PMSF], followed by centrifugation to remove the Ni-beads. The eluted proteins were then analyzed by immunoprecipitation in the presence of 1% Triton X-100 and 0.5 M NaCl with anti-12CA5 monoclonal antibody as described above.

Acknowledgments

We thank Dan Tishkoff and Pam Silver for advice on yeast genetics, Jo Jiricny for comparing portions of the MSH6 amino acid sequence to the GTBP amino acid sequence prior to publication, Brett Satterberg for construction of the plasmid pK8, Eric Alani for construction of the plasmid RDK351 and advice on immunoprecipitation of MSH2, Rick Fishel, Jean Y.J. Wang, and Nina Winand for advice on in vitro transcription and translation reactions, Sue Jinks-Robertson for the *lys2–Bgl* disruption plasmid, A. Jeyaprakash for several *S. cerevisiae* strains, Paul Morrison and Christine Earabino of the Dana-Farber Cancer Institute Molecular Biology Facility for help with DNA sequencing, James Lipford for advice on detecting mutations, and James Lipford, Paul Morrison, and Dan Tishkoff for comments on the manuscript and/or help with preparation of figures. This work was supported by National Institutes of Health grants GM50006 to R.D.K., and CA06516 and AI28691 to the Dana-Farber Cancer Institute for support of its Core Molecular Biology Facility.

The publication costs of this article were defrayed in part by payment of page charges. This article must therefore be hereby marked "advertisement" in accordance with 18 USC section 1734 solely to indicate this fact.

References

Aaltonen, L.A., P. Peltomaki, F. Leach, P. Sistonen, S.M. Pylkkanen, J.-P. Mecklin, H. Jarvinen, S. Powell, J. Jen, S.R. Hamilton, G.M. Petersen, K. W. Kinzler, B. Vogelstein, and A. de

la Chapelle. 1993. Clues to the pathogenesis of familial colorectal cancer. *Science* **260:** 812–816.

Alani, E., R.A.G. Reenan, and R. Kolodner. 1994. Mismatch repair proteins directly affect gene conversion in *Saccharomyces cerevisiae* by regulating heteroduplex tract length. *Genetics* **137:** 19–39.

Alani, E., N.-W. Chi, and R.D. Kolodner. 1995. The *Saccharomyces cerevisiae* MSH2 protein specifically binds to duplex oligonucleotides containing mismatched DNA base pairs and loop insertions. *Genes & Dev.* **9:** 234–247.

Barnes, W.M. 1994. PCR amplification of up to 35-kb DNA with high fidelity and high yield from lambda bacteriophage templates. *Proc. Natl. Acad. Sci.* **91:** 2216–2220.

Bhattacharyya, N.P., A. Skandalis, A. Ganesh, J. Groden, and M. Meuth. 1994. Mutator phenotype in human colorectal carcinoma cell lines. *Proc. Natl. Acad. Sci.* **91:** 6319–6323.

Bishop, D.K., M.S. Williamson, S. Fogel, and R.D. Kolodner. 1987. The role of heteroduplex correction in gene conversion in *Saccharomyces cerevisiae*. *Nature* **328:** 362–364.

Bishop, D.K., J. Andersen, and R.D. Kolodner. 1989. Specificity of mismatch repair following transformation of *Saccharomyces cerevisiae* with heteroduplex plasmid DNA. *Proc. Natl. Acad. Sci.* **86:** 3713–3717.

Borresen, A.-L., R.A. Lothe, G.I. Meling, S. Lystad, P. Morrison, J. Lipford, M.F. Kane, T.O. Rognum, and R.D. Kolodner. 1995. Somatic mutations in the *hMSH2* gene in microsatellite unstable colorectal carcinomas. *Hum. Mol. Genet.* **11:** 2065–2072.

Boyer, J.C., A. Umar, J. Risinger, M.F. Kane, J. Lipford, J.C. Barrett, R.D. Kolodner, and T.A. Kunkel. 1995. Microsatellite instability, mismatch repair deficiency and genetic defects in human cancer cell lines. *Cancer Res.* **55:** 6063–6070.

Bronner, C.E., S.M. Baker, P.T. Morrison, G. Warren, L.G. Smith, M.K. Lescoe, M. Kane, C. Earabino, J. Lipford, A. Lindblom, P. Tannergard, R.J. Bollag, A.R. Godwin, D.C. Ward, M. Nordenskjold, R. Fishel, R. Kolodner, and R.M. Liskay. 1994. Mutation in the DNA mismatch repair gene homolog *hMLH1* is associated with hereditary nonpolyposis colon cancer. *Nature* **368:** 258–261.

Chi, N.-W. and R.D. Kolodner. 1994. Purification and characterization of MSH1, a yeast mitochondrial protein that binds to DNA mismatches. *J. Biol. Chem.* **269:** 29984–29992.

Drummond, J.T., G.-M. Li, M.J. Longley, and P. Modrich. 1995. Mismatch recognition by an hMSH2-GTBP heterodimer and differential repair defects in tumor cells. *Science* **268:** 1909–1912.

Eschelman, J.R. and S.D. Markowitz. 1995. Microsatellite instability in inherited and sporadic neoplasms. *Curr. Opin. Oncol.* **7:** 83–89.

Eschelman, J.R., E.Z. Lang, G.K. Bowerfind, R. Parsons, B. Vogelstein, J.K.V. Wilson, M.L. Veigl, W.D. Sedwick, and S.D. Markowitz. 1995. Increased mutation rate at the hprt locus accompanies microsatellite instability in colon cancer. *Oncogene* **10:** 33–37.

Fishel, R.A., M.K. Lescoe, M.R.S. Rao, N. Copland, N. Jenkins, J. Garber, M. Kane, and R. Kolodner. 1993. The human mutator gene homolog MSH2 and its association with hereditary nonpolyposis colon cancer. *Cell* **75:** 1027–1038.

Fishel, R.A., A. Ewel, S. Lee, M.K. Lescoe, and J. Griffith. 1994. Binding of mismatched microsatellite DNA sequences by the human MSH2 protein. *Science* **266:** 1403–1405.

Grilley, M., K.M. Welsh, S.-S. Su, and P. Modrich. 1989. Isolation and characterization of the *Escherichia coli mutL* gene product. *J. Biol. Chem.* **264:** 1000–1004.

Hollingsworth, N.M., L. Ponte, and C. Halsey. 1995. *MSH5*, a novel MutS homolog, facilitates meiotic reciprocal recombination between homologs in *Saccharomyces cerevisiae* but not mismatch repair. *Genes & Dev.* **9:** 1728–1739.

Honchel, R., K.C. Halling, D.J. Schaid, M. Pittelkow, and S.N. Thibodeau. 1994. Microsatellite instability in Muir-Torre syndrome. *Cancer Res.* **54:** 1159–1163.

Ionov, Y., M.A. Peinado, S. Malkbosyan, D. Shibata, and M. Perucho. 1993. Ubiquitous somatic mutations in simple repeated sequences reveal a new mechanism for colonic carcinogenesis. *Nature* **260:** 558–561.

Jeyaprakash, A., J.W. Welch, and S. Fogel. 1994. Mutagenesis of yeast MW104-1B strain has identified the uncharacterized *PMS6* DNA mismatch repair gene locus and additional alleles of existing *PMS1, PMS2* and *MSH2* genes. *Mutat. Res.* **325:** 21–29.

Jeyaprakash, A., R. Gupta, and R. Kolodner. 1996. *Saccharomyces cerevisiae pm52* mutations are alleles of *MLH1* and *pms2-2* corresponds to an HNPCC causing missense mutation. *Mol. Cell Biol.* (in press).

Kolodner, R.D. 1995. Mismatch repair: Mechanisms and relationship to cancer susceptibility. *Trends Biochem.* **20:** 397–402.

Kolodner, R.D., N.R. Hall, J. Lipford, M.F. Kane, M.R.S. Rao, P. Morrison, L. Wirth, P.J. Finan, J. Burn, P. Chapman, C. Earabino, E. Merchant, and D.T. Bishop. 1994. Structure of the human *MSH2* locus and analysis of two Muir-Torre kindreds for *msh2* mutations. *Genomics* **24:** 516–526.

Kolodner, R.D., N.R. Hall, J.R. Lipford, M.F. Kane, P. Morrison, P.J. Finan, J. Burn, P. Chapman, C. Earabino, E. Merchant, and D.T. Bishop. 1995. Structure of the human MLH1 locus and analysis of HNPCC kindreds for mlh1 mutations. *Cancer Res.* **55:** 242–248.

Kramer, B., W. Kramer, M.S. Williamson, and S. Fogel. 1989. Heteroduplex DNA correction in *Saccharomyces cerevisiae* is mismatch specific and requires functional *PMS* genes. *Mol. Cell. Biol.* **9:** 4432–4440.

Kramer, W., B. Kramer, M.S. Williamson, and S. Fogel. 1989. Cloning and nucleotide sequence of DNA mismatch repair gene *PMS1* from *Saccharomyces cerevisiae*: Homology of PMS1 to procaryotic MutL and HexB. *J. Bacteriol.* **171:** 5339–5346.

Lea, D.E. and C.A. Coulson. 1948. The distribution of the numbers of mutants in bacterial populations. *J. Genet.* **49:** 264–248.

Leach, F.S., N.C. Nicolaides, N. Papadopoulos, B. Liu, J. Jen, R. Parsons, P. Peltomaki, P. Sistonen, L.A. Aaltonen, M. Nystrom-Lahti, X.-Y. Guan, J. Zhang, P.S. Meltzer, J.-W. Yu, F.-T. Kao, D.J. Chen, K.M. Cerosaletti, R.E.K. Fournier, S. Todd, T. Lewis, R.J. Leach, S.L. Naylor, J. Weissenbach, J.-P. Mecklin, H. Jarvinen, G.M. Petersen, S.R. Hamilton, J. Green, J. Jass, P. Watson, H.T. Lynch, J.M. Trent, A. de la Chapelle, K.W. Kinsler, and B. Vogelstein. 1993. Mutations of a mutS homolog in hereditary nonpolyposis colorectal cancer. *Cell* **75:** 1215–1225.

Li, G.-M. and P. Modrich. 1995. Restoration of mismatch repair to nuclear extracts of H6 colorectal tumor cells by a heterodimer of human MutL homologs. *Proc. Natl. Acad. Sci.* **92:** 1950–1954.

Liu, B., R.E. Parsons, S.R. Hamilton, G.M. Petersen, H.T. Lynch, P. Watson, S. Markowitz, J.K.V. Willson, J. Green, A. de la Chapelle, K.W. Kinzler, and B. Vogelstein. 1994. *hMSH2* mutations in hereditary nonpolyposis colorectal cancer kindreds. *Cancer Res.* **54:** 4590–4594.

Liu, B., M.C. Nicolaides, S. Markowitz, J.K.V. Willson, J.R. Parsons, J. Jen, N. Papadopolous, P. Peltomaki, A. de la Chapelle, S.R. Hamilton, K.W. Kinzler, and B. Vogelstein. 1995. Mismatch repair gene defects in sporadic colorectal

cancers with microsatellite instability. *Nature Genet.* **9:** 48–55.

Modrich, P. 1991. Mechanisms and biological effects of mismatch repair. *Annu. Rev. Genet.* **25:** 229–253.

———. 1994. Mismatch repair, genetic stability, and cancer. *Science* **266:** 1959–1960.

New, L., K. Liu, and G.F. Crouse. 1993. The yeast gene *MSH3* defines a new class of eukaryotic MutS homologs. *Mol. & Gen. Genet.* **239:** 97–108.

Nicolaides, N.C., N. Papadopoulos, B. Liu, Y. Wei, K.C. Carter, S.M. Ruben, C.A. Rosen, W.A. Haseltine, R.D. Fleischmann, C.M. Fraser, M.D. Adams, J.C. Venter, M.G. Dunlop, S.R. Hamilton, G.M. Petersen, A. de la Chapelle, B. Vogelstein, and K. Kinzler. 1994. Mutations of two PMS homologs in hereditary nonpolyposis colon cancer. *Nature* **371:** 75–80.

Nystrom-Lahti, M., R. Parsons, P. Sistonen, L. Pylkkanen, L.A. Aaltonen, F.S. Leach, S.R. Hamilton, P. Watson, E. Bronson, R. Fusaro, J. Cavalieri, J. Lynch, S. Lanspa, T. Smyrk, P. Lynch, T. Drouhard, K.W. Kinzler, B. Vogelstein, H.T. Lynch, A. de la Chapelle, and P. Peltomaki. 1994. Mismatch repair genes on chromosomes 2p and 3p account for a major share of hereditary nonpolyposis colorectal cancer families evaluable by linkage. *Am. J. Hum. Genet.* **55:** 659–665.

Orth, K., J. Hung, A. Gazdar, A. Bowcock, J.M. Mathis, and J. Sambrook. 1994. Genetic instability in human ovarian cancer cell lines. *Proc. Natl. Acad. Sci.* **91:** 9495–9499.

Palombo, F., P. Gallinari, I. Iaccarino, T. Lettieri, M. Hughes, A. D'Arrigo, O. Truong, J.J. Hsuan, and J. Jiricny. 1995. GTBP, a 160 kD protein essential for mismatch binding activity in human cells. *Science* **268:** 1912–1914.

Papadopoulos, N., N.C. Nicolaides, Y.-F. Wei, S.M. Ruben, K.C. Carter, C.A. Rosen, W.A. Haseltine, R.D. Fleischmann, C.M. Fraser, M.D. Adams, J.C. Venter, S.R. Hamilton, G.M. Petersen, P. Watson, H.T. Lynch, P. Peltomaki, J.-P. Mecklin, A. de la Chapelle, K.W. Kinzler, and B. Vogelstein. 1994. Mutation of a *mutL* homolog in hereditary colon cancer. *Science* **263:** 1625–1629.

Papadopoulos, N., N.C. Nicolaides, B. Liu, R.E. Parsons, C. Lengauer, F. Palombo, A. D'Arrigo, S. Markowitz, J.K.V. Wilson, K.W. Kinzler, J. Jiricny, and B. Vogelstein. 1995. Mutations of GTBP in genetically unstable tumors. *Science* **268:** 1915–1917.

Parsons, R., G.-M. Li, M.J. Longley, W.-H. Fang, N. Papadopoulos, J. Jen, A. de la Chapelle, K.W. Kinzler, B. Vogelstein, and P. Modrich. 1993. Hypermutability and mismatch repair deficiency in RER+ tumor cells. *Cell* **75:** 1227–1236.

Peltomaki, P., L.A. Aaltonen, P. Sistonen, L. Pylkkanen, J.-P. Mecklin, H. Jarvinen, J.S. Green, J.R. Jass, J.L. Weber, F.S. Leach, G.M. Petersen, S.R. Hamilton, A. de la Chapelle, and B. Vogelstein. 1993a. Genetic mapping of a locus presisposing to human colorectal cancer. *Science* **260:** 810–812.

Peltomaki, P., R.A. Lothe, L.A. Aaltonen, L. Pylkkanen, M. Nystrom-Lahti, R. Seruca, L. David, R. Holm, D. Ryberg, A. Haugen, A. Brogger, A.-L. Borresen, and A. de la Chapelle. 1993b. Microsatellite instability is associated with tumours that characterize the hereditary non-polyposis colorectal carcinoma syndrome. *Cancer Res.* **53:** 5853–5855.

Prolla, T.A., D.-M. Christie, and R.M. Liskay. 1994a. A requirement in yeast DNA mismatch repair for *MLH1* and *PMS1*, two homologs of the bacterial *mutL* gene. *Mol. Cell. Biol.* **14:** 407–415.

Prolla, T.A., Q. Pang, E. Alani, R.D. Kolodner, and R.M. Liskay. 1994b. Interactions between the MSH2, MLH1 and PMS1 proteins during the initiation of DNA mismatch repair. *Science* **265:** 1091–1093.

Reenan, R.A.G. and R.D. Kolodner. 1992a. Characterization of insertion mutations in the *Saccharomyces cerevisiae MSH1* and *MSH2* genes: Evidence for separate mitochondrial and nuclear functions. *Genetics* **132:** 975–985.

———. 1992b. Isolation and characterization of two *Saccharomyces cerevisiae* genes encoding homologs of the bacterial HexA and MutS mismatch repair proteins. *Genetics* **132:** 963–973.

Rocco, V., B. DeMassy, and A. Nicolas. 1992. The *Saccharomyces cerevisiae ARG4* initiator of meiotic gene conversion and its associated double-strand DNA breaks can be inhibited by transcriptional interference. *Proc. Natl. Acad. Sci.* **89:** 12068–12072.

Ross-Macdonald, P. and G.S. Roeder. 1994. Mutation of a meiosis-specific MutS homolog decreases crossing over but not mismatch correction. *Cell* **79:** 1069–1080.

Sherman, F., G.R. Fink, and J.B. Hicks. 1986. Yeast DNA isolations. In *Methods in yeast genetics*, pp. 125–134. Cold Spring Harbor Laboratory, Cold Spring Harbor, NY

Shibata, D., M.A. Peinado, S. Ionov, S. Malkhosyan, and M. Perucho. 1994. Genomic instability in repeated sequences in an early somatic event in colorectal tumorigenesis that persists after transformation. *Nature Genet.* **6:** 273–281.

Steele, D.F. and S. Jinks-Robertson. 1992. An examination of adaptive reversion in *Saccharomyces cerevisiae. Genetics* **132:** 9–21.

Strand, M., T.A. Prolla, R.M. Liskay, and T.D. Petes. 1993. Destabilization of tracts of simple repetitive DNA in yeast by mutations affecting DNA mismatch repair. *Nature* **365:** 274–276.

Strand, M., M.C. Earley, G.F. Crouse, and T.D. Petes. 1995. Mutations in the *MSH3* gene preferentially lead to deletions within tracts of simple repetitive DNA in *Saccharomyces cerevisiae. Proc. Natl. Acad. Sci.* **92:** 10418–10421.

Umar, A., J.C. Boyer, D.C. Thomas, D.C. Nguyen, J.I. Risinger, J. Boyd, Y. Ionov, M. Perucho, and T.A. Kunkel. 1994. Defective mismatch repair in extracts of colorectal and endometrial cancer cell lines exhibiting microsatellite instability. *J. Biol. Chem.* **269:** 14367–14370.

Williamson, M.S., J.C. Game, and S. Fogel. 1985. Meiotic gene conversion mutants in *Saccharomyces cerevisiae*. I. Isolation and characterization of *pms1-1* and *pms1-2*. *Genetics* **110:** 609–646.

Redundancy of Saccharomyces cerevisiae MSH3 and MSH6 in MSH2-dependent mismatch repair.

G T Marsischky, N Filosi, M F Kane, et al.

Genes Dev. 1996, **10:**
Access the most recent version at doi:10.1101/gad.10.4.407